Hydrographic Observations along the CODE Central Line off Northern California, 1981

ADRIANA HUYER

College of Oceanography, Oregon State University, Corvallis, OR 97331

(Manuscript received 29 August 1983, in final form 12 July 1984)

ABSTRACT

Repeated CTD observations were made along a single section spanning the continental shelf off northern California at 38°40'N during 1981. The section consisted of nine standard stations between 1 and 46 km from the shore in water depths between 40 and 1700 m. The shelf break was at a depth of 150 m about 25 km from shore. The section was occupied 17 times between 13 April and 3 August and twice in December, and a similar section had been occupied in February.

During the April–August period, winds were strong and persistently favorable for upwelling. Isotherms, isohalines and isopycnals in the upper 200 m sloped persistently upward toward the coast, and coldest, saltiest and densest surface waters almost always occurred at the most inshore station. Variations in wind strength caused changes in the surface layer over the entire shelf: stronger winds were associated with lower temperatures and higher salinities. Subsurface temperatures increased gradually between April and August. We were unable to account for most of the salinity variance during this period.

Shelf waters were considerably warmer and less saline in winter, when the wind direction and speed were highly variable. Isotherms, isohalines and isopycnals were nearly level in winter. Dynamic height and coastal sea level were high in winter and low in summer; there was good agreement between them.

1. Introduction

During spring and summer of 1981 an intensive physical oceanographic study called the First Coastal Ocean Dynamics Experiment (CODE-1) was conducted over the continental shelf of northern California (Fig. 1) between Pt. Arena and Pt. Reyes (CODE Group, 1983). The primary purpose was to improve our understanding of the response of continental shelf waters to a time-varying wind stress. Because our primary interest was in the temporal variability, the CODE program included repeated CTD observations along the CODE-1 Central Line. These repeated sections extended seaward beyond the moored array and down to 1000 m over the continental slope—they thus provide a distinct viewpoint for studying the variability of coastal waters. The CODE-1 CTD observations were most concentrated during three two-week "hydro" legs on the R.V. *Wecoma:* 25 April–7 May, 16–29 May and 1–14 July 1981 (Fleischbein *et al.,* 1982a; Gilbert *et al.,* 1982a; Olivera *et al.,* 1982). Additional CTD measurements were made on the mooring deployment and recovery cruises of 10–14 April and 1–4 August 1981 (Gilbert *et al.,* 1981, 1982b). During each of these cruises, we occupied nine standard stations (Table 1) spanning the continental shelf and upper slope along the Central Line at least twice, for a total of seventeen repeated sections between 13 April and 3 August 1981. On some occasions, the section extended farther out to sea. The same nine stations were also repeated twice in December 1981 (Fleischbein *et al.,* 1982b) and a similar section with slightly different station positions (Fig. 1) had been occupied in February 1981 (Fleischbein *et al.,* 1981).

At each station, a Neil Brown Mark III-B CTD was lowered at about 45 m min^{-1} to a maximum depth of 1000 m, or within ~20 m of the bottom over the upper continental slope and within ~5 m of the bottom over the shelf. Processing the CTD data included correcting the conductivity data to agree with *in situ* calibration samples, filtering to correct for differences in time constants between sensors, and averaging into 1 or 2 db intervals (Gilbert *et al.,* 1981). Accuracy of the final processed pressure, temperature and salinity data is believed to be ±2 db, ±0.01°C and ±0.003‰, respectively.

Coastal sea level was measured continuously by tide gages at Arena Cove (38°55.2'N, 123°43.2'W) and Pt. Reyes (37°59.5'N, 122°58.5'W). The data were recorded once per hour, adjusted for the "inverted barometer effect" by adding 1 cm for every 1 mb increase in atmospheric pressure, and low-pass filtered (half-power point at 40 h) to remove tidal signals.

Winds were measured continuously at the Pt. Arena Coast Guard Station (38°57'N, 123°44'W) and, since 1 April 1981, at a permanent buoy (Number 46013) maintained at 38°14'N, 123°18'W by the National Data Buoy Office. Fluctuations in wind and wind stress are qualitatively similar at the two locations, but the buoy winds are consistently stronger

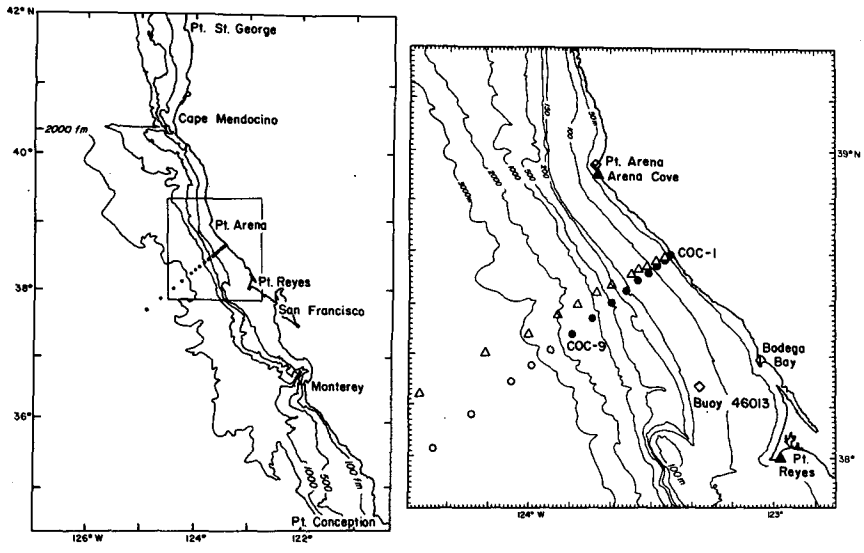

FIG. 1. Location of the CODE-1 study area (left) and station positions along the CODE Central Line (right). Closed circles show stations repeated 17 times during CODE-1 (April–August 1981) and twice during December 1981; stations farther from shore (open circles) were occupied occasionally. Open triangles show stations occupied in February 1981. Also shown are permanent anemometers (diamonds) and coastal tide gages (solid triangles).

and appear to be a better representation of the wind field over the water (cf. Mills and Beardsley, 1983; Halliwell and Allen, 1983). Thus, the wind data from NDBO Buoy 46013 are used for quantitative comparisons with the CTD data. Since this buoy was not in operation in early 1981, the Pt. Arena winds are used to discuss the seasonal variations. The winds were recorded once per hour at the buoy, and once every three hours (interpolated to hourly values) at the Coast Guard Station. The hourly data were low-pass filtered (half-power point at 40 h) and rotated counterclockwise by 10.9° at Pt. Arena and by 50° at Buoy 46013 into their local principal axes. At both locations, the variance of the alongshore (major axis) component exceeds the variance of the onshore (minor axis) component by a factor of 10.

Between the end of March and early September, the alongshore component of the wind was predominantly southeastward (Fig. 2). In contrast, winds were predominantly poleward during February and December. The distributions of temperature, salinity and density anomaly (sigma-theta) for all of the Central Line sections (Fig. 3) show that: 1) temperature generally decreases with depth while salinity increases with depth; 2) isotherms, isohalines and isopycnals are generally parallel on a given date; 3) isopleths over the continental shelf slope upward toward the coast between 13 April and 13 July but they are roughly level in winter; 4) the temperature (8–9°C) and salinity (33.8–34.0‰) bands that outcrop near the coast in spring and early summer lie at depths of 150–200 m in winter; 5) waters over the continental shelf are coldest in spring and warmest in winter; 6) there is more variability near the surface than near the bottom over the continental shelf; and 7) the variability of the near-surface layer extends well beyond the shelf. These and other features will be discussed more fully in the following sections.

TABLE 1. Nominal positions for each station along the CODE-1 Central Line, average distance from shore ($\bar{x}$), average water depth ($\bar{Z}_B$), and the maximum common pressure (P_{max}).

Station name	Latitude (North)	Longitude (West)	$\bar{x}$ (km)	Z_B (m)	P_{max} (db)
COC-1	38°39.8′	123°25.5′	1.1	41	29
COC-2	38°38.8′	123°26.9′	3.8	76	69
COC-3	38°37.5′	123°28.9′	7.3	93	87
COC-4	38°36.2′	123°30.8′	11.0	109	103
COC-5	38°34.6′	123°33.3′	15.8	136	125
COC-6	38°32.7′	123°36.2′	21.3	149	140
COC-7	38°30.3′	123°39.6′	27.8	382	298
COC-8	38°27.1′	123°44.5′	37.2	1181	1001
COC-9	38°24.0′	123°49.2′	46.2	1697	1001

2. Structure and variability during CODE-1: April–August

Winds during CODE-1 were predominantly alongshore in the equatorward direction (Fig. 2), i.e., favorable for coastal upwelling, and they were generally strong. Wind and wind stress were also very persistent: low-passed winds were unfavorable for upwelling less than 10% of the time. During the 120-day period from 8 April to 5 August, the mean alongshore wind at Buoy 46013 was -8.7 m s^{-1}; the mean alongshore wind stress was about -1.7 dyn cm^{-2}. These winds would result in a seasonal mean offshore Ekman transport of 1.9×10^3 kg s^{-1} m^{-1}, larger than in two of the upwelling regions described

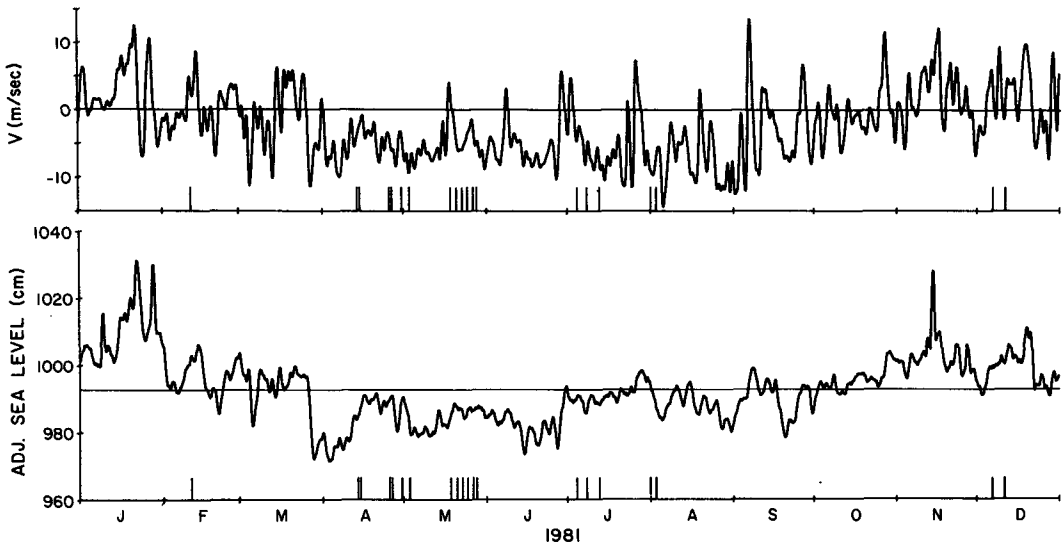

FIG. 2. Time series of the alongshore component (toward 349°T) of the low-passed wind at Pt. Arena Coast Guard Station and of low-passed adjusted sea level at Arena Cove; the 1981 mean adjusted sea level is 993.0 cm. Vertical bars show the times of CTD observations along the CODE Central Line.

by Smith (1981), but smaller than in the third (0.5×10^3 kg s^{-1} m^{-1} off Oregon, 1.3×10^3 kg s^{-1} m^{-1} off Peru, and 2.8×10^3 kg s^{-1} m^{-1} off NW Africa).

a. The mean fields

The average and standard deviation of temperature, salinity and sigma-theta were calculated from the 17 CODE-1 stations. All of the mean isopleths between the surface and 200 m slope upward toward the coast (Fig. 4): surface waters are coldest, most saline and densest at the closest inshore station, and warmest, least saline and lightest at the farthest offshore station. Inshore surface salinities exceeding 33.9‰ indicate that water normally upwells from depths of about 150 m; it sometimes upwells from depths of about 250 m (compare 11–12 February and 13 April in Fig. 3). These depths are greater than those observed in the upwelling regions off Oregon (e.g., Halpern, 1974) and Peru (Brink *et al.*, 1983) where the mean Ekman transport is relatively small, but about the same as in the upwelling region off Northwest Africa (Barton *et al.*, 1977) where the mean Ekman transport is large.

The fact that surface waters are coldest and saltiest at the closest inshore station, only 1 km from shore, suggests that the strongest upwelling occurs in a narrow band immediately adjacent to the coast. This extreme inshore location of the zone of strongest upwelling may be related to the shelf geometry: most of the shelf is relatively flat and deep, and only a very narrow (<2 km) coastal strip is less than 60 m deep. Densest surface waters and strongest upwelling also occur adjacent to the coast of central Oregon (Halpern, 1974, 1976) where the shelf is also quite deep. In comparison, the wide continental shelf off Northwest Africa is very shallow—the 50 m isobath is about 15 km from the coast, and coldest surface waters and strongest upwelling there occurs over the midshelf (Barton *et al.*, 1977).

Can simple two-dimensional upwelling account for the observed mean offshore gradients? If we make the simple assumption that both mean offshore Ekman transport of 1.9×10^3 kg s^{-1} m^{-1} and mean downward surface heat flux of 180 W m^{-2} (Nelson and Husby, 1983) are uniformly distributed through the surface mixed layer, we obtain an offshore surface temperature gradient of about 0.2°C per 10 km, only about half of the observed surface temperature gradient (Fig. 4). Since there is almost no mean evaporation or precipitation in this region (Nelson and Husby, 1983) we also fail to account for the observed mean salinity gradient of about 0.2‰ per 10 km. These strong mean gradients may be maintained partly by an onshore eddy heat and salt flux, as they are off Oregon (Bryden *et al.*, 1980).

The mean isopycnals in the upper 200 m slope upward toward the coast, roughly parallel to the isotherms and isopycnals. These are consistent with coastal upwelling, but they also indicate the presence of a mean vertical shear in the alongshore flow, with currents at the surface more strongly southward (or more weakly northward) than those below. Isopycnal slopes decrease gradually to zero at about 400 m, indicating the vertical shear disappears at about this depth.

b. The variability

The distributions of the standard deviations (Fig. 4) show that the variability is greatest in the surface layers. Salinity varies least over the inner shelf where

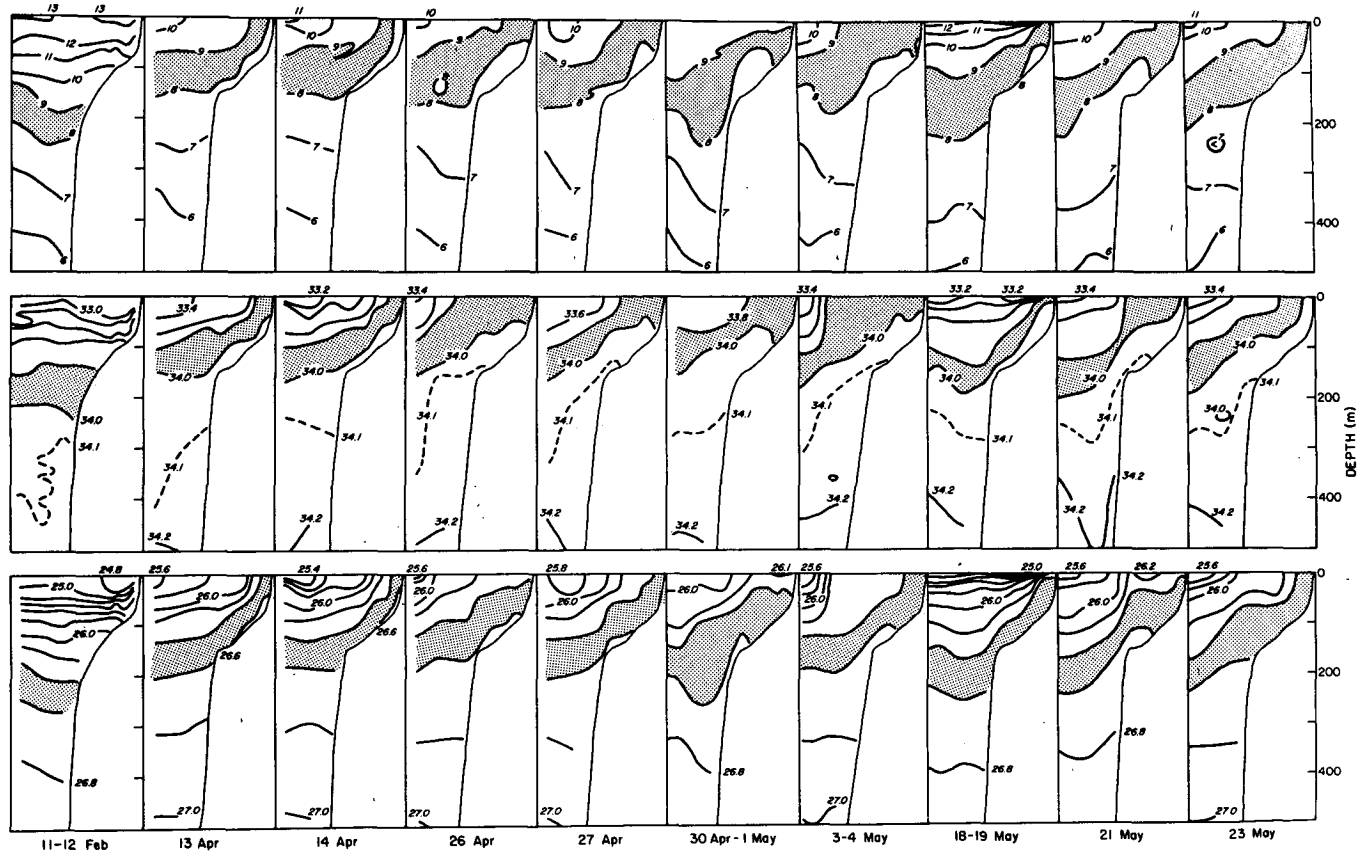

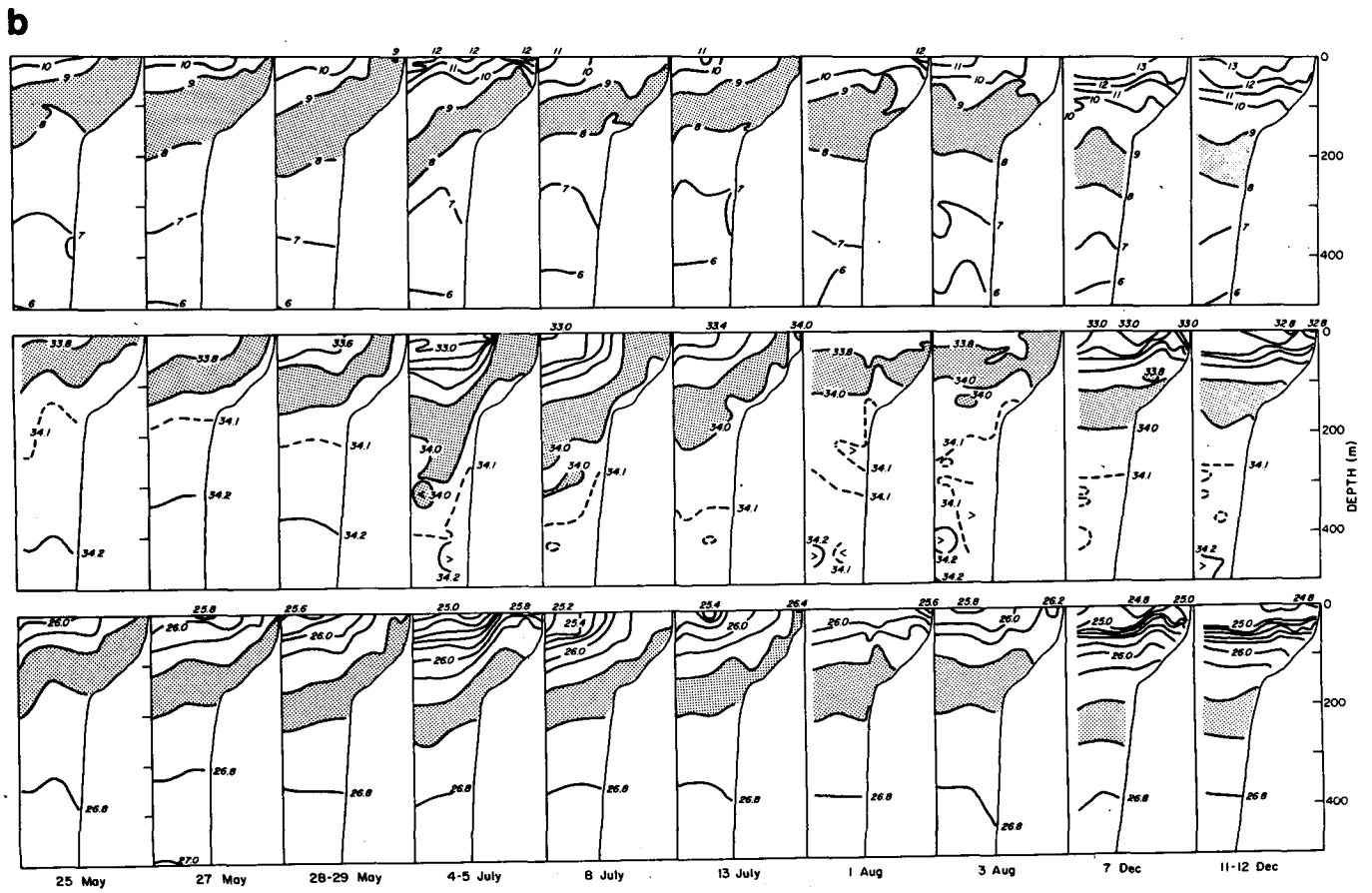

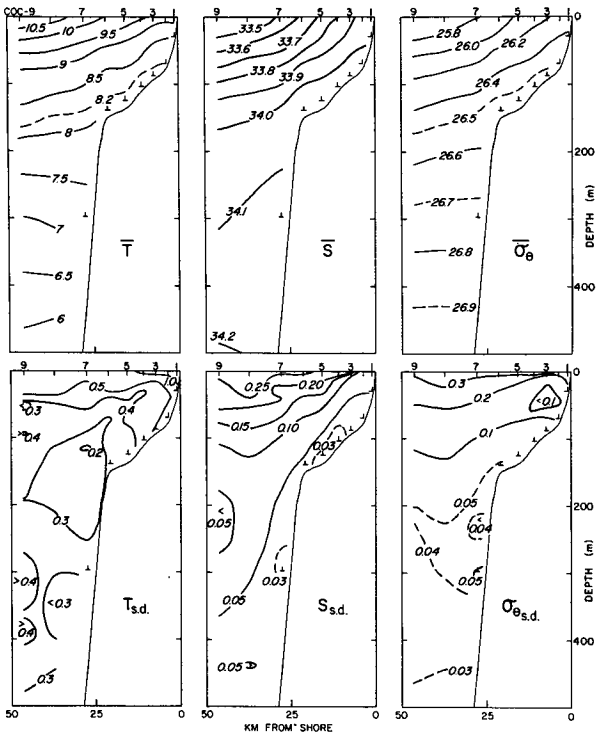

FIG. 4. The distributions of the average and standard deviations of temperature, salinity and sigma-theta calculated from the 17 CTD sections between 13 April and 3 August 1981.

temperature varies most. Both temperature and salinity are quite variable over the outer shelf and upper slope.

To see if this variability was associated with changes in the local wind stress we first examined temperature sections made during periods of variable winds (Fig. 5). Suitable sequences were obtained on three occasions (Fig. 2); in each case, the first section was made during relatively weak winds and later sections were made during stronger, upwelling-favorable winds. The first sequence began after three weeks of continuously equatorward winds: on 26 April the equatorward wind exceeded 5 m s^{-1} and waters over the continental shelf were relatively cool, between 7 and 10°C. Winds were stronger on 27 April but the temperature structure was similar. The wind decreased to 5 m s^{-1} on 29 April, and surface temperatures were >9°C over the entire shelf during the 30 April–1 May section. Equatorward winds increased to more than 10 m s^{-1} during this section and remained steady through the 3–4 May section when the entire shelf was colder than 9°C and inshore waters were colder than 8.5°C. Although maximum winds were about the same during the sections of 27 April and 3–4 May, shelf temperatures were substantially lower during the latter, apparently because of the difference in winds during the preceding days (~7 m s^{-1} on 26 April and ~13 m s^{-1} on 2–3 May).

The second sequence began late on 18 May, just after a day of weak upwelling-unfavorable winds: although surface temperatures were warm (>12°C) over most of the shelf, subsurface isotherms still sloped up toward the coast. On 21 May, after two days of increasing upwelling-favorable winds, the 12°C isotherm had disappeared and the 10°C isotherm was beyond the shelf break. Continuing strong winds through 23 May brought little change. Decreasing winds again brought warmer water close to shore on 27 May. Bottom temperatures increased gradually during this sequence; they were apparently unaffected by changes in wind strength.

The third sequence, which began on 4 July, shows the same qualitative results as the other two (Fig. 5). All three sequences show that bottom and very nearshore properties change gradually, independent of variations in the local wind. They also show that surface layer properties over and beyond the continental shelf respond directly to changes in the wind: surface temperatures decrease when the strength of the upwelling-favorable wind increases, lagging the wind by about a day. Surface temperatures increased (and surface salinities over the outer shelf decreased) when the wind strength decreased, even when the wind direction remained favorable for upwelling. This suggests that the surface waters move shoreward when upwelling-favorable winds decrease, even though coastal upwelling continues. A similar relaxation of the surface temperature field during weakening equatorward winds was observed in the upwelling region off Northwest Africa (Barton *et al.*, 1977).

To examine the variability in a more objective way, we calculated the structure and time-dependence of empirical orthogonal modes (Kundu *et al.*, 1975) of each of the temperature, salinity and sigma-theta fields. In this technique, a correlation matrix is calculated from all observations of a given variable at particular sampling points: the modes are the eigenvectors of this correlation matrix and the eigenvalues give the variance associated with each mode. There are as many eigenvectors (modes) as the original number of sampling points, and the modes are ordered by their contribution to the total variance; there is no correlation among the modes. Usually only a few modes account for most of the variance and the other modes can be neglected.

We used two different schemes to subsample the continuous hydrographic data before calculating the empirical modes. The first scheme (designated "odd")

FIG. 3. Vertical–offshore distribution of temperature, salinity and sigma-theta along the Central Line during 1981: (a) 11 February–23 May; (b) 25 May–12 December. Each panel shows the distribution for the upper 500 m within 50 km of the coast. The same temperature (8–9°C), salinity (33.8–34.0‰) and sigma-theta (26.4 to 26.6) bands are shaded throughout.

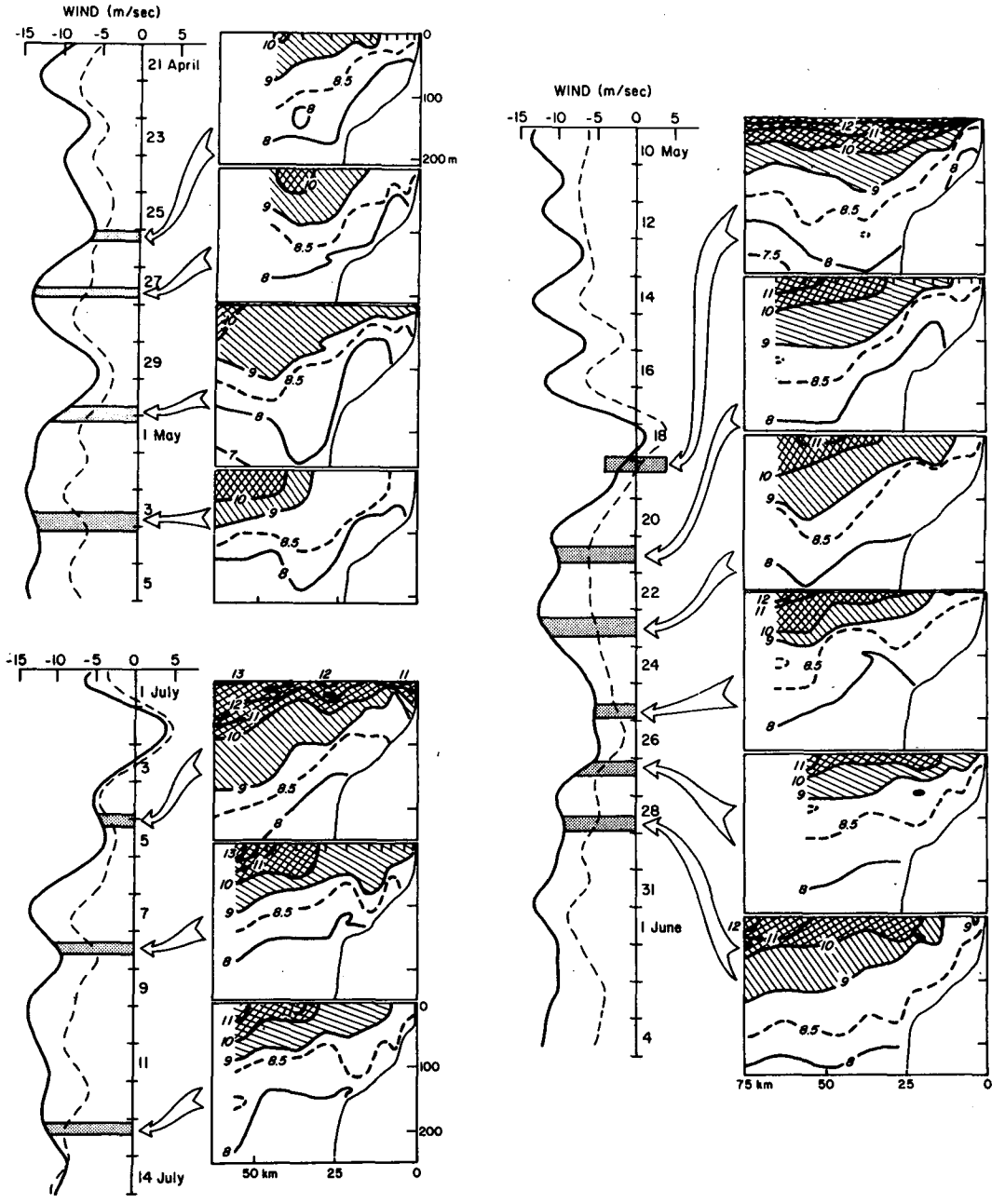

FIG. 5. Sequences of repeated temperature sections with the low-passed alongshore component of the wind at Buoy 46013 (solid) and at Pt. Arena (dashed), during periods of variable winds: 21 April–5 May, 10 May–4 June and 1–14 July 1981.

was designed to examine the overall vertical and offshore structure in the upper 100 m, and the second scheme (designated "shelf") was designed to examine the structure over the shelf in more detail. The sampling points for each scheme are indicated in Fig. 6. In both cases, the first mode of each variable accounted for more than half of the total variance, while the second mode accounted for less than a quarter of the variance; hence, only the first modes of each variable are discussed here.

The spatial distributions of the amplitude (eigenvector times the square root of corresponding eigenvalue) of these modes are shown in Fig. 6. The first "odd" mode of temperature (T_o) has no zero-crossings and largest amplitudes occur at the surface near shore; it resembles the distribution of the standard deviation (Fig. 4) and implies that offshore temperature variations are in phase with those over the inner shelf. The first "shelf" temperature (T_s) mode also has largest amplitudes at the surface over the inner

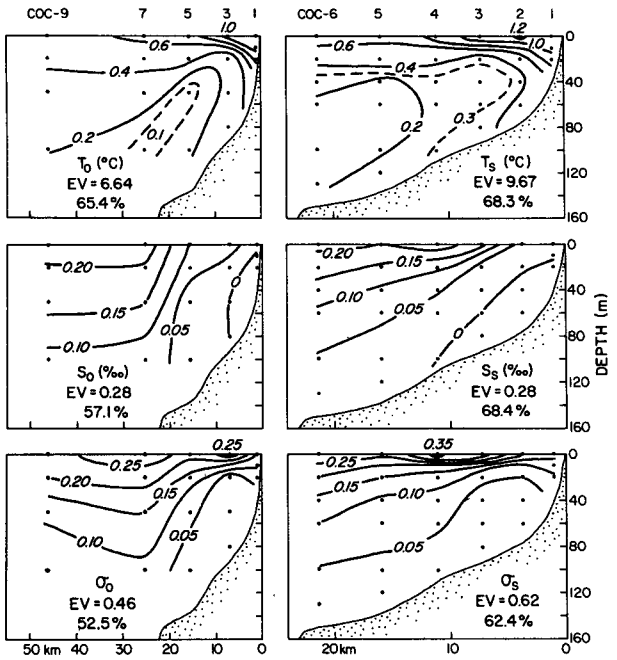

FIG. 6. The vertical and offshore structure, the eigenvalue (EV), and the percentage of total variance of the first empirical orthogonal modes of temperature, salinity and sigma-theta: the "odd" modes (left) and the "shelf" modes (right).

shelf; in addition, it suggests there is associated temperature variability in the bottom and near-shore boundary layers. The "odd" and "shelf" temperature modes are very highly correlated ($r^3 = 0.98$), and thus appear to represent the same phenomenon. The "odd" salinity mode (S_o) contains mainly offshore salinity fluctuations over the continental slope and shelf, and the "shelf" salinity mode (S_s) has strongest amplitudes over the outer shelf, with very little variability near shore and near the bottom. The "shelf" and "odd" salinity modes are not highly correlated ($r^3 = 0.49$) and thus do not represent exactly the same phenomenon. The "odd" mode of density (σ_o) has weak offshore gradients but strong vertical gradients, particularly over the midshelf. The "shelf" density mode (σ_s) also has largest amplitudes at the surface over the midshelf, and it is well correlated with the "odd" density mode ($r^2 = 0.83$). There is little correlation between the respective temperature and salinity modes [$r^2(T_o, S_o) = 0.08$ and $r^2(T_s, S_s) = 0.15$], and temperature and salinity fluctuations contribute about equally to the density variations: $r^2(\sigma_o, T_o) = 0.58$; $r^2(\sigma_o, S_o) = 0.64$; $r^2(\sigma_s, T_s) = 0.65$; and $r^2(\sigma_s, S_s) = 0.71$.

Time variations of the amplitude of each mode were compared with the variations in wind, wind stress, adjusted sea level and day-number (Table 2). Comparisons with the low-passed wind and wind stress data were made using both values (V_o, τ_o) that are simultaneous with each section, and values (V_{18}, τ_{18}) that preceded each section by 18 hours. (Preliminary comparisons of low-passed temperature time series from the CODE-1 moored array to wind and wind stress data showed a broad correlation peak at lags between 0 and 36 h, and the local inertial frequency is 19 h.) All of the comparisons have 15 degrees of freedom if all 17 CTD sections are independent samples; the corresponding significance levels are given in Table 2. All of the modes were slightly better correlated with the alongshore wind than with the alongshore wind stress (Table 2); this was consistent with preliminary analysis of temperature data from the moored array. The difference may not be significant, and may reflect the fact that even the currently accepted method of calculating wind stress from hourly velocity measurements (i.e., following Large and Pond, 1981) does not estimate the actual wind stress with sufficient accuracy. Nevertheless, in the remainder of this section, we shall restrict our attention to comparisons with wind rather than wind stress. There was generally better correlation with the wind preceding each section by 18 hours (V_{18}) than with the simultaneous wind (V_o), but even these wind data account for only about 50% of "shelf" density mode, and 30% of the two temperature modes (Table 2). The "odd" salinity mode does not seem to be correlated with the wind at all. Both temperature modes are quite strongly correlated with day-number, i.e., with time elapsed during CODE-1. Together, wind and day-number account for about 75% of the variance of each temperature mode. The temperature modes also seem to be correlated with adjusted sea level, but sea level itself is weakly correlated with both wind and day-number (Table 2). Thus further comparisons of the hydrographic fields are limited to the preceding wind (V_{18}) and day-number.

Since the empirical modes did not clearly extract the wind-driven portion of the variability, we also calculated simple linear correlation and regression coefficients between V_{18} and the CTD data at selected depths (indicated in Figs. 7 and 8). The resulting distributions (Fig. 7) of correlation (r^2) and regression

TABLE 2. Linear correlation coefficients (r^2) between the first "odd" and first "shelf" modes of temperature (T), salinity (S) and sigma-theta and other variables: the simultaneous low-passed alongshore wind (V_o) and wind stress (τ_o), the preceding wind (V_{18}) and wind stress (τ_{18}), the day-number (DN) and the adjusted sea level (η) at Pt. Arena. Assuming 7, 10, or 15 degrees of freedom, the 95% significance level is 0.34, 0.25 or 0.17, respectively.

	V_o	τ_o	V_{18}	τ_{18}	DN	η
T_o	0.17	0.15	0.23	0.20	0.45	0.36
S_o	0.13	0.10	0.04	0.01	0.00	0.00
σ_o	0.33	0.24	0.28	0.17	0.09	0.09
T_s	0.15	0.12	0.23	0.19	0.49	0.36
S_s	0.34	0.24	0.36	0.24	0.00	0.00
σ_s	0.40	0.29	0.48	0.33	0.11	0.12
V_o	—	0.93	0.72	0.60	0.00	0.17
V_{18}	—	0.61	—	0.88	0.01	0.20
DN	—	0.00	—	0.01	—	0.22

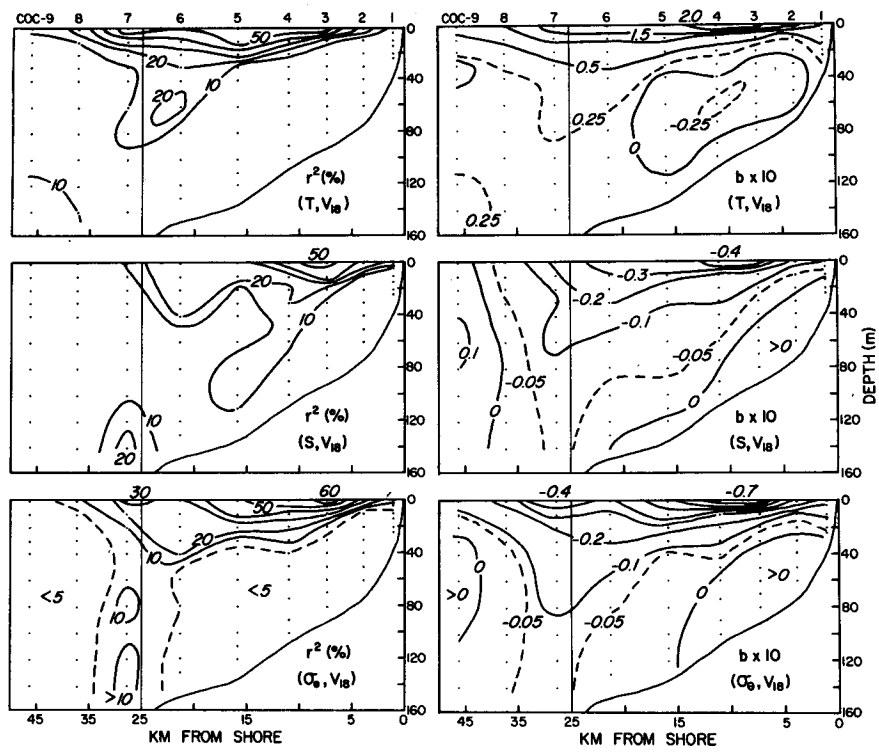

FIG. 7. Correlation and regression coefficients between temperature, salinity and sigma-theta at selected depths, and the preceding wind, V_{18}.

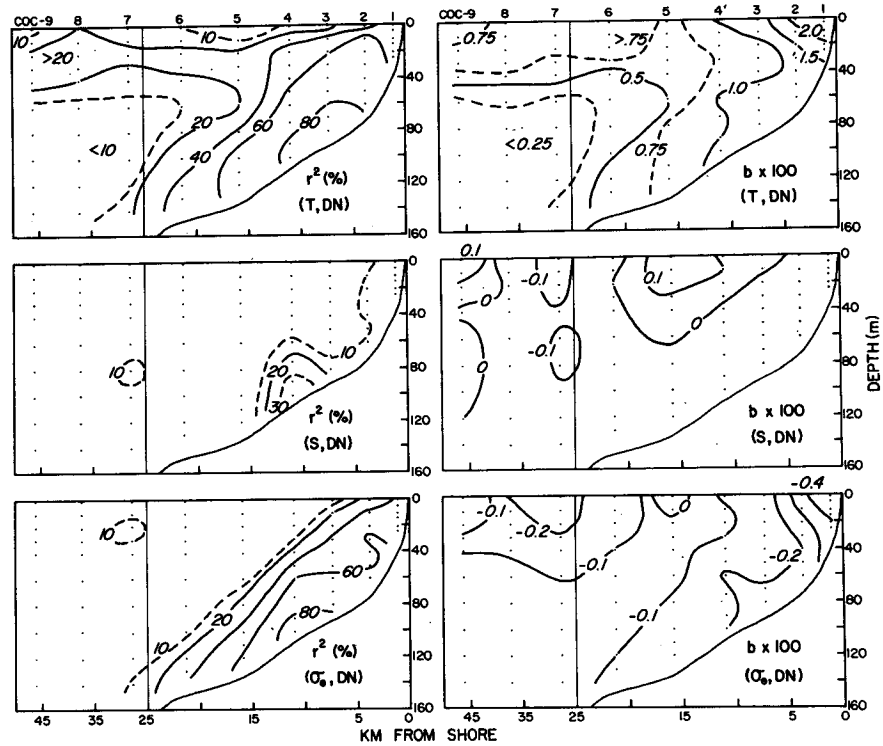

FIG. 8. Correlation and regression coefficients between temperature, salinity and sigma-theta at selected depths, and the day-number, DN.

(*b*) coefficients show that variations in wind strength cause changes in the surface layer over the entire shelf; these changes are restricted to about the upper-third of the water over the shelf. The wind also seems to cause surface temperature changes beyond the shelf break, but it does not cause the surface salinity changes that occur there (cf. Figs. 6, 7). The wind seems to induce some subsurface variability near the shelf break, but it accounts for less than 20% of the variability there. Figure 7 also suggests that the depth of the layer influenced by the wind increases from about 10 m inshore to about 60 m over the shelf break. A positive change in the wind (i.e., a decrease in the strength of the upwelling-favorable wind) results in higher surface temperatures, and lower surface salinities and densities, over the entire shelf. There is a hint that temperature in the bottom boundary layer also increases when upwelling weakens.

A similar regression analysis of these variables on day-number (Fig. 8) shows that a linear trend with time accounts for more than 60% of the near-bottom temperature and density variance over much of the continental shelf. In contrast, there is no significant trend in the salinity anywhere (Fig. 8). The warming trend amounts to more than a degree per 100 days near the bottom over the inner shelf and it is quite obvious in the temperature data (Fig. 9); it is strongest near shore where initial temperatures are coldest. Over most of the shelf, this warming trend accounts for a larger fraction of the temperature and density variance than the wind: only in the surface layer does the wind dominate.

Since values of the V_{18} and day-number are very nearly uncorrelated ($r^2 = 0.01$), they may be treated as independent variables: i.e., the r^2 value of the multiple correlation is just the sum of the separate r^2 values shown in Figs. 7 and 8. Thus, together, the wind and day-number account for more than 50% of the temperature and density variance of the water over the inner shelf (within 10 km from shore). Except in the surface layer over the midshelf, they do not account for more than a third of the salinity variance.

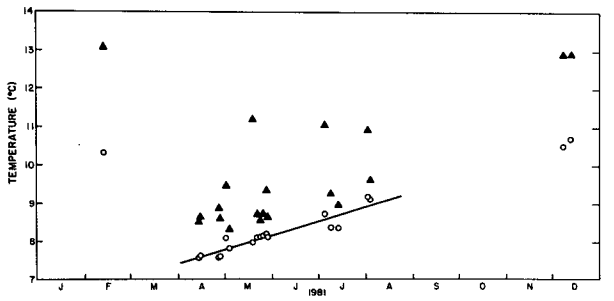

FIG. 9. The time-dependence of the temperature of the surface layer (solid dots) and the bottom layer (open dots) at COC-3, near midshelf. The sloping line is the regression of bottom-layer temperature on day-number calculated from the April–August data.

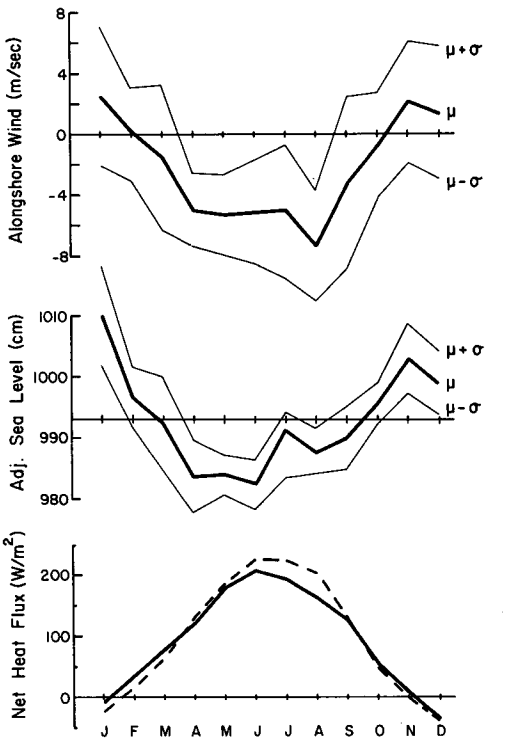

FIG. 10. The 1981 monthly means (μ) and standard deviations (σ) of the alongshore wind and adjusted sea level at Arena Cove. Also shown are monthly values of the long-term mean heat flux at 38°N, 123°W (solid) and 39°N, 124°W (dashed). (From Nelson and Husby, 1983.)

The details of the physical processes represented by these two sources are not entirely clear. The portion of the variability associated with changes in the wind is not simply due to pure two-dimensional time-dependent coastal upwelling and downwelling cycles, which would cause surface salinities to continue increasing and surface temperatures to continue decreasing as long as alongshore winds remained equatorward. With heating and wind-generated mixing at the surface, surface temperatures would eventually reach a steady state in which the cooling due to upwelling balances the surface heating (de Szoeke and Richman, 1981); however, surface salinities would continue to increase since there is virtually no precipitation at this time of the year. The increase in surface temperatures and the decrease in surface salinities associated with a decrease in strength of continued upwelling-favorable winds must result from some other process: perhaps onshore eddy diffusion, alongshore advection, or acceleration due to onshore or alongshore pressure gradients set up by the preceding strong winds.

The linear warming trend may in part result from the seasonal surface heat flux which is positive (i.e., downward) throughout the April to August period (Fig. 10). With a spatially uniform wind stress, vertical mixing would be strongest where the stratification is

weakest, i.e., over the inner shelf (Fig. 4). Mixing processes due to surface waves and bottom stress would also be strongest near shore. Thus downward mixing of the surface heat flux might explain the general structure of the observed warming trend (Fig. 8). Since warmer waters have lower density, it would also account for the density trend.

3. Seasonal variations

Although the sections were not distributed evenly throughout the year, we can make some preliminary inferences about the seasonal changes in water properties along the Code Central Line. Figures 2 and 3 suggest there were basically two different seasons: winter and spring–summer. During the winter months (January to March, October to December), the alongshore wind was highly variable with small monthly means, and sea level was above its 1981 mean (Fig. 10). During the spring–summer months (April–August), the wind was persistently equatorward and sea level was below the mean. All of the CODE-1 sections discussed above were within the spring–summer season, and the February and December sections were within the winter season.

The three winter sections are very similar to each other: in each case the isotherms, isohalines and isopleths are nearly level and parallel (Fig. 3). The thermocline and halocline are at about the same depth; together they contribute to a strong pycnocline that extends across the continental shelf and upper slope at about 50 m. Shelf waters in winter are warmer, less saline and less dense than during any of the spring–summer sections (Fig. 3). The seasonal cycle in temperature is highly asymmetrical: temperatures fall from a February high to a minimum in April and increase gradually from April through August (Fig. 9); they also rise between August and December. The similarity of the December and February temperatures is consistent with the very small winter heat flux through the surface at this location (Fig. 10). The cooling between February and April is not consistent with the surface heat flux; it is more likely associated with the seasonal onset of upwelling-favorable (equatorward) winds and with the seasonal drop in coastal sea level (Fig. 10).

If the seasonal cycle in the adjusted sea level at Pt. Arena is due to changes in the density field and if the ocean is in hydrostatic balance, the adjusted sea level data should be in reasonable agreement with the dynamic height of the sea surface ($\Delta D_{0/p}$) relative to an appropriate isobaric surface. This dynamic height is just the integral of the specific volume anomaly between the surface and the reference level p. For each CTD section, we calculated $\Delta D_{0/500}$: at stations deeper than 500 db it was calculated directly from the CTD data at that station; in water shallower than 500 db, we used the extrapolation technique described by Reid and Mantyla (1976) whereby $\Delta D_{p/500}$ is calculated by linear extrapolation from the next offshore pair of stations and $\Delta D_{0/p}$ is calculated directly from the CTD data. Figure 11 shows very good agreement between $\Delta D_{0/500}$ at COC-1 and the adjusted sea level at Pt. Arena: the correlation is high, and the slope of the regression line is very nearly one. The largest deviation from the line is about 6 cm; errors due to the extrapolation procedure, uncertainties in position and isopycnal displacements due to internal waves can easily account for deviations of this magnitude. Thus, we cannot reject the hypothesis that changes in the height of sea level at the coast are due entirely to density changes in the upper 500 db. At COC-8, the bottom depth exceeds 100 m, and $\Delta D_{0/500}$ can be calculated directly from the CTD data, without any extrapolation. Values of $\Delta D_{0/500}$ at COC-8 are still correlated with sea level at Arena Cove, but the regression coefficient is only 0.65 (Fig. 11). Interpreting $\Delta D_{0/500}$ as the sea-surface height at both COC-1 and COC-8, this implies that sea level variations have an offshore decay scale that is greater than the shelf width: the amplitudes at COC-8, 37 km from shore, are about ⅔ of those at the coast.

Comparisons with sea level were repeated for the dynamic height of the surface relative to 1000 db.

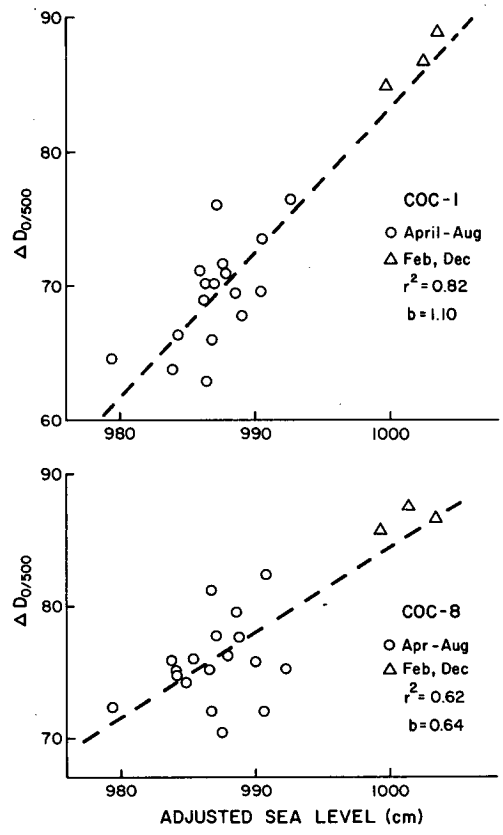

FIG. 11. Comparison of the dynamic height relative to 500 db at COC-1 and COC-8 with adjusted sea level at Arena Cove, showing the linear regression lines and the values of the slope (b) and the correlation coefficient (r^2).

Results for COC-8 were very similar, with both correlation and regression coefficients essentially unchanged ($r^2 = 0.66$, $b = 0.66$). Results for COC-1 yielded a regression coefficient even closer to one ($b = 1.06$) but a somewhat smaller correlation coefficient ($r^2 = 0.69$): errors associated with onshore extrapolation seem to be larger for deeper reference levels. Most of the variation in dynamic height seems to be seasonal in nature: at COC-1 the winter values are more than 15 dyn cm higher than the April–August mean (Fig. 11), in good agreement with the seasonal cycle of sea level at Arena Cove (Fig. 10). If the three winter sections are eliminated from these comparisons, only the correlation at COC-1 remains barely significant ($r^2 = 0.34$); this is consistent with the poor correlation between the CODE-1 density modes and sea level (Table 2).

4. Discussions and conclusions

The region between Pt. Arena and Pt. Reyes where the Coastal Ocean Dynamics Experiment was conducted has the strongest upwelling-favorable winds in the entire California Current system (Huyer, 1983): the spring–summer seasonal mean alongshore wind stress here exceeds the comparable values off central Oregon, Northwest Africa and Peru, the sites of previous intensive upwelling studies (Smith, 1981). These very strong winds are reflected in the maps of sea surface temperature off California issued weekly by the National Weather Service which consistently show a surface temperature minimum at the coast between Pt. Arena and Pt. Reyes (L. Breaker, personal communication, 1983). Although offshore surface temperatures far (~500 km) from the coast increase southwards at the rate of about 1°C per 100 km (Robinson, 1976), the minimum inshore surface temperatures (<8°C) in this region are actually slightly lower than those observed in the upwelling region off central Oregon, 650 km to the north. The annual mean dynamic height of 76 dyn cm at the coast (estimated from the 1981 mean adjusted sea level at Arena Cove and Fig. 11) is lower than any other value along the entire eastern shore of the North Pacific Ocean (Reid and Mantyla, 1976). Thus, the mean conditions described here are from an exceptional rather than a typical stretch of the North American west coast.

During April–August 1981, coastal winds in the region between Pt. Arena and Pt. Reyes were persistently favorable for upwelling, and wind speeds were variable but generally strong, frequently exceeding 10 m s^{-1}. The mean temperature, salinity and density sections during April–August all show isopleths sloping upward toward the coast over the continental shelf. Both mean and individual sections show that surface waters were coldest, most saline and densest at the closest inshore station, and warmest, least saline and least dense at the farthest offshore station. Although local winds continued to be strong and favorable for upwelling between April and August, the continued upwelling did not lead to continued cooling over the shelf.

The variability of the local alongshore wind stress during April–August 1981 was greater than in upwelling regions studied previously. The standard deviation of the alongshore wind stress exceeded those for the upwelling regimes off Oregon and Northwest Africa (Smith, 1981) by 50% and 25% respectively, but it was still smaller than the mean wind stress. The variations in strength of the persistent upwelling-favorable winds resulted in changes in surface-layer properties across the entire shelf: when the wind increased, the surface temperature decreased and surface salinity increased; when the wind decreased, the surface temperature increased and surface salinity decreased. Empirical orthogonal analysis showed considerable spatial coherence in the hydrographic variability: the first mode of each variable accounted for more than 60% of the variance over the shelf. Offshore temperature and density fluctuations were in phase with those over the inner and midshelf; most of the salinity variability was over and beyond the shelf-break. Regression analysis showed that the local wind accounted for half of the surface temperature and density variance and about a third of the surface salinity variance over the shelf; the wind did not account for any of the salinity variance beyond the shelf. It also showed that a warming trend between April and August accounted for more than half of the temperature and density variance of the deep water over the shelf; there was no significant trend in water properties beyond it. Together, local wind and day-number account for about half of the temperature and density variance over the shelf; we were unable to account for most of the observed salinity variance.

Although only three CTD sections were made during winter months, comparison of these with April–August sections indicates a real seasonal difference in water properties between winter and spring–summer. Isotherms, isohalines and isopycnals sloped upward toward the coast in spring and summer but they were nearly level in winter. Shelf waters were warmest and least saline in winter when the wind was highly variable and sea level was high. Subsurface waters over the shelf were coldest in spring soon after the seasonal onset of persistent equatorward winds. Comparison between coastal sea level and dynamic height at CTD stations 1 and 37 km from shore indicates that the offshore decay scale of these seasonal changes is greater than the width of the continental shelf (25 km).

Acknowledgments. I wish to thank all those who participated in obtaining the CTD data in the windy CODE region during 1981: the assistance and dedication of the officers and crew of the R.V. *Wecoma* were invaluable. I am especially grateful to R.

Schramm for setting up and maintaining the CTD system, J. Fleischbein for the preparation of several data reports, and W. E. Gilbert for assistance in analyzing the data and designing the figures. The wind and sea level data were provided by J. Allen, G. Halliwell and H. Pittock. This paper has benefited from discussions with R. Smith, D. Enfield, J. Allen, R. Beardsley and R. Davis.

This analysis and the CTD data collection were supported by the National Science Foundation through Grant OCE-8014943. This is a contribution of the Coastal Ocean Dynamics Experiment.

REFERENCES

Barton, E. D., A. Huyer and R. L. Smith, 1977: Temporal variation in the hydrographic regime near Cabo Corviero in the northwest African upwelling region, February to April 1974. *Deep-Sea Res.*, **24,** 7–23.

Brink, K. H., D. Halpern, A. Huyer and R. L. Smith, 1983: The physical environment of the Peruvian upwelling system. *Progress in Oceanography,* Vol. 12, Pergamon, 285–305.

Bryden, H. L., D. Halpern and R. D. Pillsbury, 1980: Importance of eddy heat flux in a heat budget for Oregon coastal waters. *J. Geophys. Res.*, **85,** 6649–6653.

CODE Group, 1983: Coastal Ocean Dynamics Experiment (CODE): A preliminary program description. *Eos, Trans. Amer. Geophys. Union,* **64,** 538–540.

de Szoeke, R. A., and J. G. Richman, 1981: The role of wind-generated mixing in coastal upwelling. *J. Phys. Oceanogr.*, **11,** 1534–1547.

Fleischbein, J., W. E. Gilbert, R. Schramm and A. Huyer, 1981: CTD Observations off Oregon and California, 5–17 February 1981. Oregon State University Ref. 81-16, School of Oceanography, 122 pp.

——, —— and A. Huyer, 1982a: Hydrographic Data From the First Coastal Ocean Dynamics Experiment: R/V WECOMA, Leg 4, 25 April–7 May 1981. School of Oceanography Ref. 82-2, Oregon State University, 149 pp.

——, ——, —— and R. L. Smith, 1982b: CTD Observations off Oregon and California: R/V WECOMA W8112A-B, 4–16 December 1981. School of Oceanography Ref. 82-14, Oregon State University, 80 pp.

Gilbert, W. E., A. Huyer and R. Schramm, 1981: Hydrographic Data from the First Coastal Ocean Dynamics Experiment: R/V WECOMA, Leg 2, 10–14 April 1981. School of Oceanography Ref. 81-12, Oregon State University, 34 pp.

——, J. Fleischbein, A. Huyer and R. Schramm, 1982a: Hydrographic Data from the First Coastal Ocean Dynamics Experiment: R/V WECOMA, Leg 5, 16–29 May 1981. School of Oceanography Ref. 82-5, Oregon State University, 178 pp.

——, A. Huyer and R. Schramm, 1982b. Hydrographic Data from the First Coastal Ocean Dynamics Experiment: R/V WECOMA, Leg 10, 1–4 August 1981. School of Oceanography Ref. 82-9, Oregon State University, 44 pp.

Halliwell, Jr., G. R., and J. S. Allen, 1983: CODE-1: Large-scale wind and sea level observations. *CODE-1 Moored Array and Large-Scale Data Report,* Tech. Rep. WHOI-83-23, L. K. Rosenfeld, Ed., Woods Hole Oceanographic Institution, 186 pp.

Halpern, D., 1974: Variations in the density field during coastal upwelling. *Tethys,* **6,** 363–374.

——, 1976: Structure of a coastal upwelling event observed off Oregon during July 1973. *Deep-Sea Res.*, **23,** 495–508.

Huyer, A., 1983: Coastal upwelling in the California Current system. *Progress in Oceanography,* Vol. 12, Pergamon, 259–284.

Kundu, P. K., J. S. Allen and R. L. Smith, 1975: Modal decomposition of the velocity field near the Oregon coast. *J. Phys. Oceanogr.*, **5,** 683–704.

Large, W. S., and S. Pond, 1981: Open ocean momentum flux measurements in moderate to strong winds. *J. Phys. Oceanogr.*, **11,** 324–336.

Mills, C. A., and R. C. Beardsley, 1983: CODE-1: Coastal and moored meteorological observations. *CODE-1 Moored Array and Large-Scale Data Report,* Tech. Rep. WHOI-83-23, L. K. Rosenfeld, Ed., Woods Hole Oceanographic Institution, 186 pp.

Nelson, C. S., and D. M. Husby, 1983: *Climatology of Surface Heat Fluxes over the California Current Region.* NOAA Tech Rep. NMFS SSRF-763. U.S. Dept. Commerce, Natl. Ocean. Atmos. Admin., Natl. Marine Fish. Serv., 155 pp.

Olivera, M., W. E. Gilbert, J. Fleischbein, A. Huyer and R. Schramm, 1982. Hydrographic Data from the First Coastal Ocean Dynamics R/V WECOMA, Leg 7, 1–14 July 1981. School of Oceanography Ref. 82-8, Oregon State University, 170 pp.

Reid, J. L., and A. W. Mantyla, 1976: The effect of geostrophic flow upon coastal sea elevations in the northern North Pacific Ocean. *J. Geophys. Res.*, **81,** 3100–3110.

Robinson, M. K., 1976: *Atlas of North Pacific Ocean: Monthly Mean Temperatures and Mean Salinities of the Surface Layer.* Ref. Publ. 2. Naval Oceanographic Office, Washington, D.C. 173 pp.

Smith, R. L., 1981: A comparison of the structure and variability of the flow field in three coastal upwelling regions: Oregon, Northwest Africa and Peru. *Coastal Upwelling,* F. A. Richards, Ed., Amer. Geophys. Union. Washington, DC.